Biomaterials 30 (2009) 4249–4259

Contents lists available at ScienceDirect

Biomaterials

journal homepage: www.elsevier.com/locate/biomaterials

Endocytic carboxylated nanodiamond for the labeling and tracking of cell division and differentiation in cancer and stem cells

Kuang-Kai Liu [a], Chi-Ching Wang [a], Chia-Liang Cheng [b], Jui-I Chao [a,c,*]

[a] Molecular Anticancer Laboratory, Department of Biological Science and Technology, National Chiao Tung University, Hsinchu 30068, Taiwan
[b] Department of Physics, National Dong Hwa University, Hualien 97401, Taiwan
[c] Institute of Molecular Medicine and Bioengineering, National Chiao Tung University, Hsinchu 30068, Taiwan

ARTICLE INFO

Article history:
Received 12 March 2009
Accepted 28 April 2009
Available online 4 June 2009

Keywords:
Nanodiamond
Cancer cell
Stem cell
Endocytosis
Mitosis
Differentiation

ABSTRACT

Nanodiamond (ND) is carbon nanomaterial developing for biological applications in recent years. In this study, we investigated the location and distribution of 100 nm carboxylated ND particles in cell division and differentiation. ND particles were taken into cells by macropinocytosis and clathrin-mediated endocytosis pathways. However, the cell growth ability was not altered by endocytic ND particles after long-term cell culture for 10 days in both A549 lung cancer cells and 3T3-L1 embryonic fibroblasts. ND particles were equal separating into two daughter cells of cell division approximately. Finally, the cell retained a single ND's cluster in cytoplasm after sub-cultured for several generations. Interestingly, ND's clusters were carried inside of cell but without inducing damages after long-term cell culture. Moreover, ND particles did not interfere with the gene or protein expressions on the regulation of cell cycle progression and adipogenic differentiation. Together, these findings provide that endocytic ND particles are non-cytotoxic in cell division and differentiation, which can be applied for the labeling and tracking of cancer and stem cells.

1. Introduction

Nanoparticles have been intensively evaluated for biomedical applications. Manipulation of nanoparticles is applied for both diagnostic and therapeutic applications [1–4]. Nanodiamond (ND) is a promising carbon nanomaterial developing for bio-applications in recent years. ND particles can emit bright fluorescence without photobleaching [5,6]. In addition to fluorescence property, the property of ND spins can be applied for nanoscale imaging as a scanning probe magnetometer [7,8]. Furthermore, the modified ND's surfaces provide platforms to conjugate with bio-molecules [9–11]. However, the location and distribution of ND particles in cell division and differentiation for the tracking of cancer and stem cells remain unknown.

The size, shape, and surface modifications may influence nanoparticles uptake into cells [12]. Cells utilize various endocytic mechanisms, including phagocytosis, macropinocytosis, clathrin-dependent endocytosis, caveolae-dependent uptake, and non-clathrin/noncaveolae endocytosis [13]. Phagocytosis is restricted by specialized cells such as macrophages and monocytes, which execute to clear large pathogens (e.g. bacteria). The assembly of actin filament (F-actin) mediates the formation of cell-surface ruffling and extension for filopodia formation is required for phagocytosis [13,14]. Like phagocytosis, F-actin assembly and filopodia formation need for macropinocytosis [13]. Furthermore, all mammalian cells use clathrin-dependent endocytosis to obtain essential nutrients, such as cholesterol and iron [15]. The clathrin-cage assembly is required for clathrin-dependent endocytosis [13]. The structural organization of caveolae is mediated by caveolin, a dimeric protein that binds cholesterol [16,17]. In addition to the above endocytosis mechanisms, the clathrin- and caveolae-independent pathways are discovered when cells can take into foreign molecules by disruption of clathrin or caveolin [13].

In this study, we investigated possible endocytic mechanisms of 100 nm ND particles in cancer and stem cells. ND particles can be taken into cells by both macropinocytosis and clathrin-mediated endocytosis. Moreover, endocytic ND's clusters are carried in cytoplasm and do not interfere with the normal cellular functions including cell division and differentiation.

* Corresponding author at: Department of Biological Science and Technology, National Chiao Tung University, 75 Bo-Ai Street, Hsinchu 30068, Taiwan. Fax: +886 3 5556219.
E-mail address: jichao@faculty.nctu.edu.tw (J.-I. Chao).

0142-9612/$ – see front matter © 2009 Elsevier Ltd. All rights reserved.
doi:10.1016/j.biomaterials.2009.04.056

2. Materials and methods

2.1. Preparation of carboxylated ND

The carboxylated ND particles were prepared as described recently [11]. The nominal 100 nm ND powder was from Diamond Innovations (Worthington, OH). Briefly, 0.2 g powders of ND particles were added into 15 mL acid mixture of H_2SO_4:HNO_3 (3:1) in ultrasonic bath for 24 h, then in 0.1 M NaOH aqueous solution at 90 °C for 2 h, finally in 0.1 M HCl aqueous solution at 90 °C for 2 h. Thereafter, the treated ND particles were washed with distilled water and at high speed centrifugation for several times to collect the sediment and dry. After drying, these particles were dissolved in distilled water. ND particles were ultrasonic for 20 min at room temperature before use. Importantly, the samples need to be freshly prepared.

2.2. Cell culture

A549 lung epithelial cell line was derived from the lung adenocarcinoma of a 58-year-old Caucasian male. RKO and HCT116 were colon carcinoma cell lines. BFTC905 cells were derived from bladder carcinoma. MCF-7 was a breast cancer cell line. 3T3-L1 was a fibroblast cell line derived from mouse. A549, BFTC905, MCF-7 cells were maintained in RPMI-1640 medium (Invitrogen Co., Carlsbad, CA). RKO and 3T3-L1 cells were cultured in DMEM medium (Invitrogen). HCT116 cells were maintained in McCoy's 5A medium. The complete media were supplemented with 10% FBS. These cells were cultured at 37 °C and 5% CO_2 in a humidified incubator (310/Thermo, Forma Scientific, Inc., Marietta, OH).

2.3. Bio-atomic force microscopy (Bio-AFM)

To measure ND interacting and binding with cell membrane, A549 cells were cultured on coverslips and then treated with ND particles. The cells were analyzed by a bio-atomic force microscope (NanoWizard, JPK Instruments, Berlin). Bio-AFM was mounted on an inverted microscope, TE-2000-U (Nikon, Japan). Silicon nitride non-sharpened cantilevers used had a nominal force constant of 0.06 N/m (DNP-20, Veeco). Imaging was performed using contact mode. Line scan rates varied from 0.5 to 2 Hz.

2.4. Transmission electron microscopy (TEM)

After treatment of ND particles, the cells were harvested and washed with phosphate buffer (pH 7.4) and then fixed with 2.5% glutaraldehyde for 1 h at 4 °C. The cells were washed with 5% sucrose (in PBS) for 15 min twice at 4 °C. Then the cells were fixed by 1% osmium tetroxide at room temperature for 1 h, and washed with 5% sucrose in PBS for 15 min twice at 4 °C. Thereafter, the cells were washed by ddH_2O for 15 min four times, and then stained with 2% uranyl acetate for 1 h at room temperature. Cells were dehydrated in graded series of ethanol (final in 100% ethanol) for 10 min. The sample was incubated with 100% ethanol for 15 min twice and replaced with incubation at acetone for 15 min. Finally, the sample was embedded in Spurr's resin (Electron microscopy science). Ultra-thin cross sections (Leica EMUC6) (~80 nm) of cells were observed under a TEM (HITACHI H-7500).

2.5. Confocal microscopy

The cells were cultured on coverslips, which were kept in a 35-mm Petri dish for 16–20 h before treatment. After treatment with or without NDs, the cells were washed with isotonic PBS (pH 7.4), and then were fixed with 4% paraformaldehyde solution in PBS for 1 h at 37 °C. The coverslips were washed three times with PBS, and non-specific binding sites were blocked in PBS containing 10% FBS, 0.3% Triton X-100 for 1 h. The cells were incubated with mouse anti-clathrin (1:100) (Millipore) antibody in PBS containing 10% FBS for overnight at 4 °C. Thereafter, the cells were washed three times with 0.3% Triton X-100 in PBS. Subsequently, the cells were incubated with goat anti-mouse Cy3 (1:50) in PBS containing 10% FBS for 2.5 h at 37 °C. Cytoskeleton of β-tubulin proteins was stained with anti-β-tubulin Cy3 (1:50) for 30 min at 37 °C. The nuclei or chromosomes were stained with Hoechst 33258. After staining, the samples were examined under a Leica confocal laser scanning microscope (Mannheim, Germany) that equipped with a UV laser (351/364 nm), an Ar laser (457/488/514 nm), and an HeNe laser (543 nm/633 nm).

2.6. Cell cycle analysis

To examine the effect of ND on the cell cycle progression, the cells were plated at a density of 1×10^6 cells per p60 dish in complete medium for 16–20 h. The cells were treated with or without 100 μg/mL ND particles for 48 h, and then re-cultured in fresh medium for cell cycle analysis by every 2 days until total 10 days. At the end of incubation, the cells were collected and fixed with ice-cold 70% ethanol overnight at −20 °C. Thereafter, the cell pellets were incubated with 4 μg/mL PI solution containing 1% Triton X-100 and 100 μg/mL RNase for 30 min. To avoid cell aggregation, the cell solutions were filtered through nylon membrane (BD Biosciences, San Jose, CA). A minimum of ten thousand cells in each samples were analyzed by

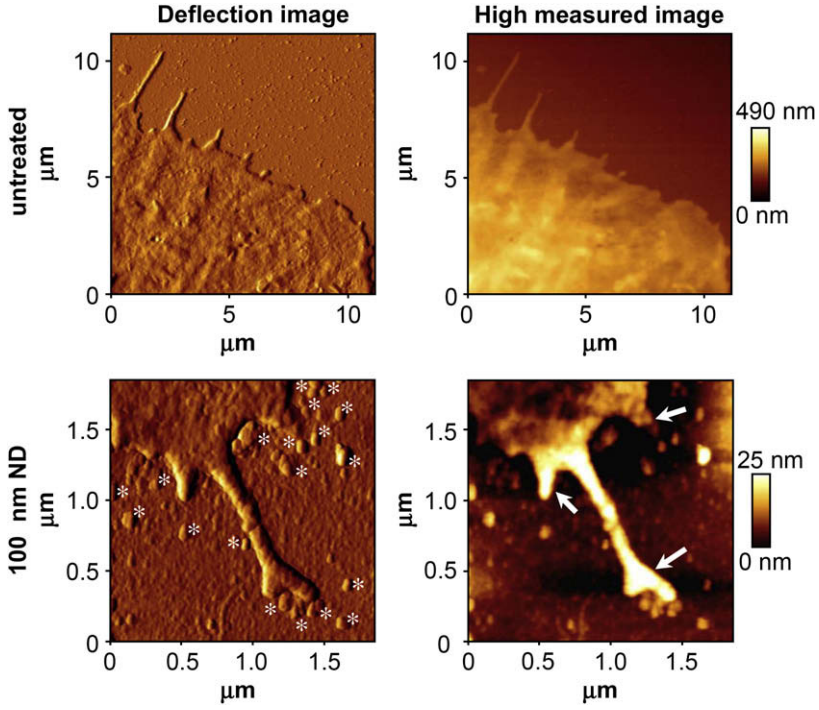

Fig. 1. Interaction of ND particles and cell membrane observed by bio-atomic force microscope (Bio-AFM). A549 cells were cultured on the coverslips in 35-mm Petri dish. The cells were treated with or without 100 nm ND particles (100 μg/mL for 4 h) and were observed by Bio-AFM. The deflection images of Bio-AFM show the contour of an A549 cell membrane surrounding. The upper pictures were from an ND-untreated A549 cell. The arrows indicated filopodia formed from cell membrane extension (lower pictures). The ND's particles (the stars, lower pictures) were taken into the ruffling and invagination of cell membrane.

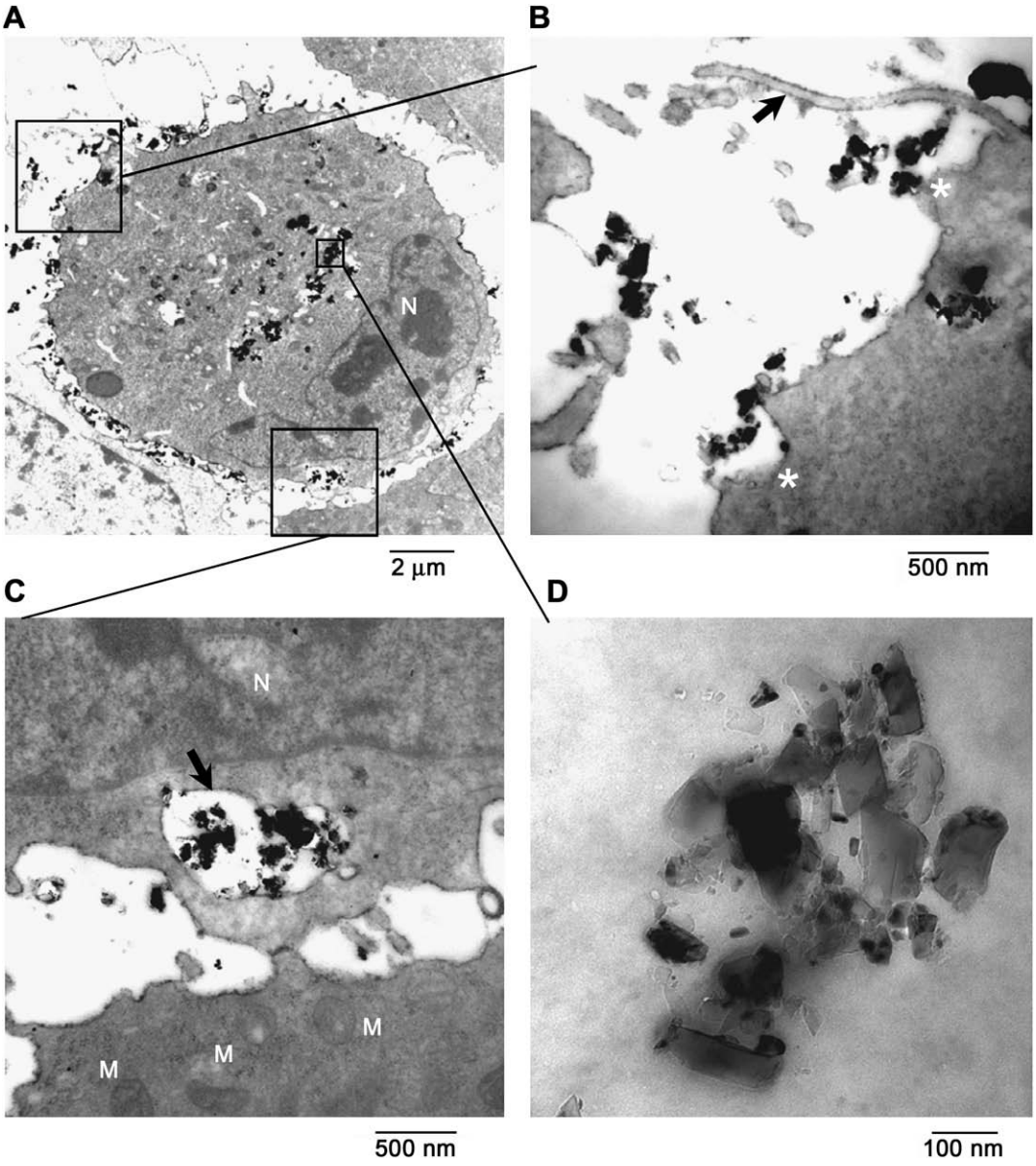

Fig. 2. Location and distribution of ND particles observed by transmission electron microscope (TEM). A549 cells were treated with 100 nm ND particles (100 μg/mL for 4 h). At the end of treatment, the cells were fixed 2.5% glutaraldehyde and analyzed by TEM. (A) ND particles were ingested into an A549 cell or surrounding in the cell membrane (dark black spots). (B) The morphology of macropinocytosis by a filopodium (the arrow) of cell membrane extension was formed for ND's entrance. The stars indicated cell membrane ruffling and invagination were formed for ND's uptake. N indicated the location of cell nucleus. M indicated the location of mitochondria. (C) An endocytic vesicle of ND particles was formed inside of cell (the arrow). (D) The amplify picture showed several ND particles accumulated to a single ND's cluster.

a CellQuest software in flow cytometer (BD Biosciences). The percentage of each cell cycle phase was quantified by a ModFit LT software (Ver. 2.0, BD Biosciences).

2.7. Cell growth assay

A549 or 3T3-L1 cells were plated at a density of 1×10^6 cells per p100 Petri dish in complete medium for 16–20 h. Then the cells were treated with or without 100 μg/mL NDs for 48 h. After treatment with ND particles, the cells were re-cultured in fresh medium for counting total cell number by every 2 days until total 10 days.

2.8. Western blot analysis

At the end of treatment, the cells were lysed in the ice-cold whole cell extract buffer containing the protease inhibitors. Total protein extracts were prepared for Western blot analysis using specific CDC2 (Calbiochem, San Diego, CA), cyclin B1 (Calbiochem), phospho-CDC2 (threonine-161) (Cell Signaling Technology, Inc., Beverly, MA), cyclin D1 (Santa Cruz Biotechnology, Inc., Santa Cruz, CA), and actin (Millipore) antibodies. Briefly, equal amounts of proteins in samples were subjected to electrophoresis using 10% sodium dodecyl sulfate-polyacrylamide gels. After electrophoretic transfer of proteins onto polyvinylidene fluoride membranes, they were sequentially hybridized with primary antibody and followed with a horseradish peroxidase-conjugated second antibody (Santa Cruz Biotechnology). Finally, the protein bands were visualized followed by detection with a chemiluminescence kit (PerkinElmer Life and Analytical Sciences, Boston, MA).

2.9. Adipogenic differentiation

To induce adipogenic differentiation, 3T3-L1 cells were plated at a density of 1×10^6 cells per 100-mm Petri dish in DMEM medium with 10% calf serum. After cell growing confluent, the cells were treated with differentiated medium, which supplemented with 0.5 mM isobutyl-1-methylxanthine (Sigma Chemical Co., St. Louis, MO), 1 μM dexamethasone (Sigma), 10 ng/mL insulin (Sigma), 50 μM indomethacin (Sigma), 1 μM roseglitazone (GlaxoSmithKline) and 10% FBS. Adipogenic differentiation was determined by the accumulation of neutral lipid vacuoles in cells. The differentiated fat cells were fixed with 4% paraformaldehyde for 1 h and then stained with oil-red O (Sigma–Aldrich) for 30 min.

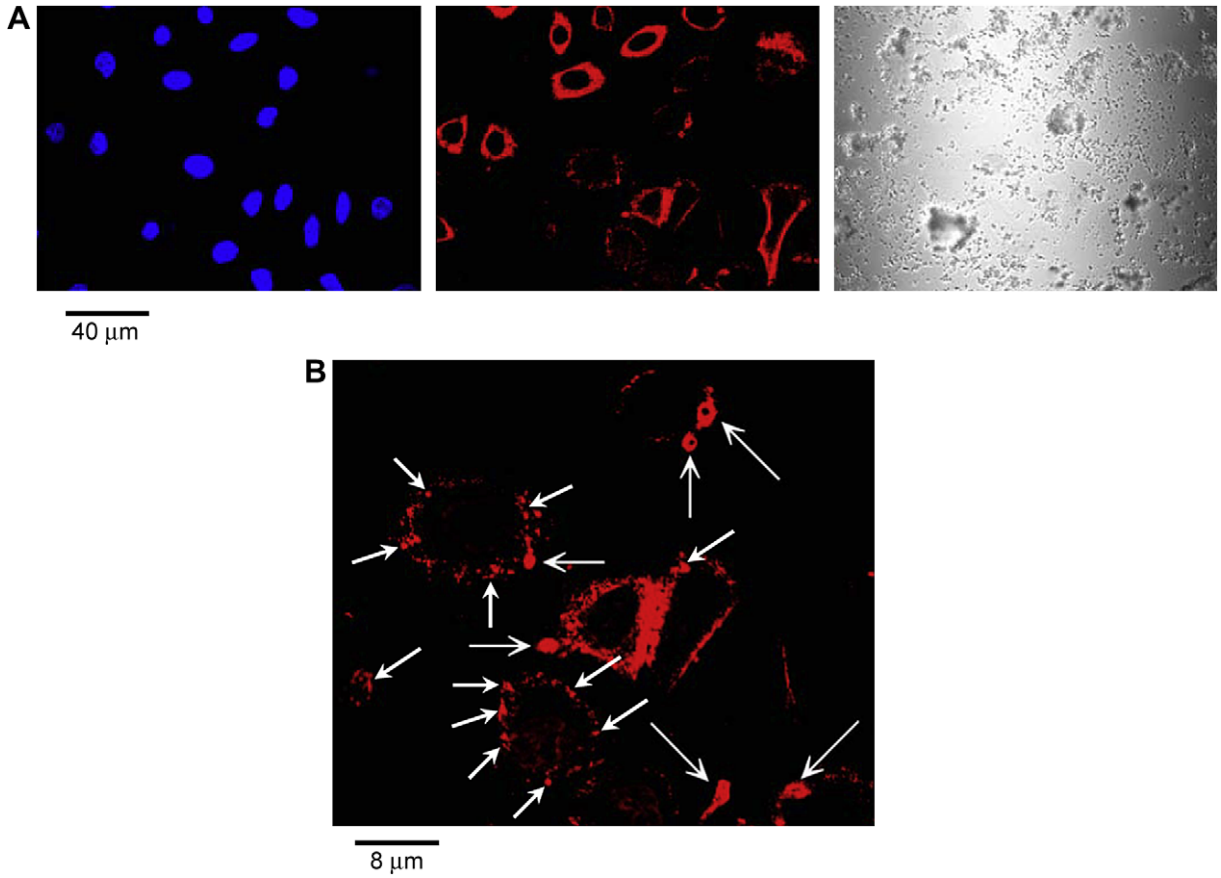

Fig. 3. Protein expression and vesicle formation of clathrin in ND-treated cells. A549 cells were incubated with or without 100 μg/mL ND particles for 4 h. At the end of treatment, the cells were subjected to nuclear and clathrin staining analyzed by a laser scanning confocal microscope. The cells were incubated with mouse anti-clathrin antibody and then incubated with goat anti-mouse Cy3. The red color indicated the location of clathrin proteins. The nuclei were stained with Hoechst 33258 that presented with blue color. Clathrin vesicles (the arrows) were formed around the membranes of A549 cells.

2.10. Reverse transcription-polymerase chain reaction (RT-PCR)

Cells were plated at a density of 1–2 × 10^6 cells per 60-mm Petri dish in culture medium. Total cellular RNA was purified by TRIzol (Invitrogen) according to the manufacturer's protocol. RNA concentrations were determined by spectrophotometry. cDNAs were synthesized by Moloney murine leukemia virus (M-MLV) reverse transcriptase with oligo $(dT)_{15}$ primer (Promega, Madison, WI). Each reverse transcript was amplified with actin as an internal control. The following primer pairs were used for amplification: adiponectin: 5′-ATGCTACTGTTGCAAGCTCT-3′ and 5′-CACCCTTAGGACCAAGAAG-3′; PPARγ: 5′-ATGGGTGAAACTCTGGGAGA-3′ and 5′-CAACTGTGGTAAAGGGCTTG-3′; actin: 5′-TGTATTCCCCTCCATCGTGG-3′ and 5′-CTCTTTGATGTCACGCACGATTTC-3′. RT-PCR was performed by a DNA thermal cycler, 5331/Mastercycler gradient (Eppendorf, Hamburg, Germany). The initial denaturation was performed at 94 °C for 2 min, followed by 30 cycles at 94 °C for 15 s, 55 °C

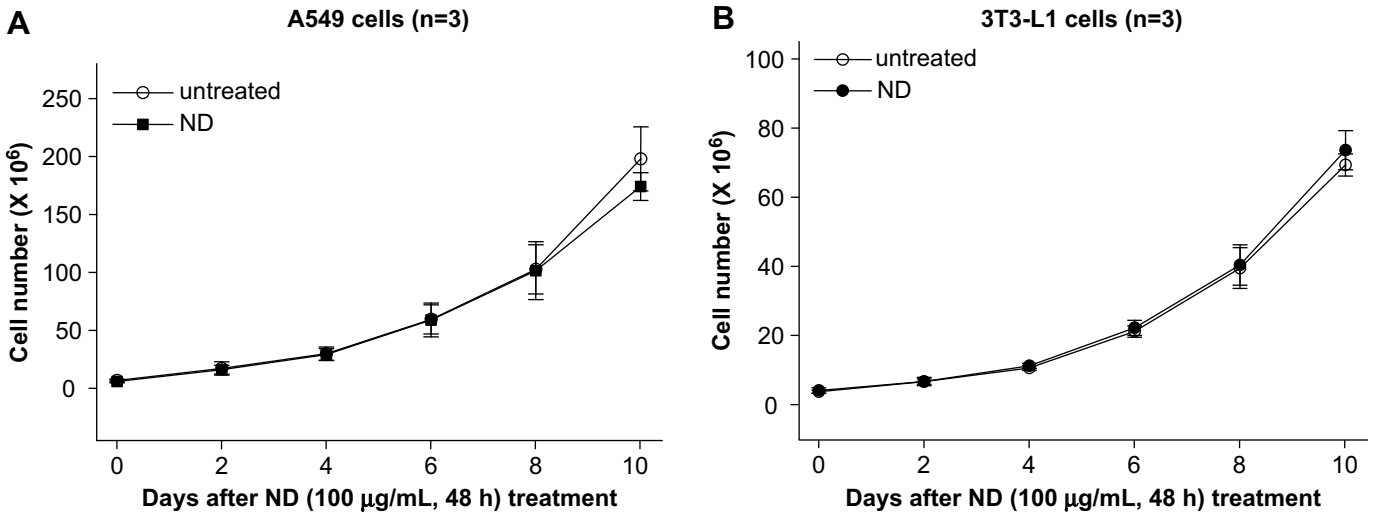

Fig. 4. The long-term effect of ND on the long-term cell growth ability in A549 and 3T3-L1 cells. (A) A549, and (B) 3T3-L1 cells were treated with or without 100 nm ND particles (100 μg/mL for 48 h), and the cells were re-cultured in fresh medium for counting the total cell number by every 2 days until total 10 days. Results were obtained from 3 separate experiments and the *bar* represents the mean ± S.E.

for 15 s, and 72 °C for 30 s; and 72 °C for 2 min. The PCR products were visualized on 2% agarose gels with ethidium bromide staining under UV transillumination, and photograph was taken by a camera (Ezcatcher, Medclub Scientific Co., Taipei, Taiwan).

3. Results

3.1. ND particles are taken into the cells by macropinocytosis and clathrin-mediated endocytosis

A549 is a human lung cancer epithelial cell. The endocytic process of ND particles in A549 cells was observed by bio-atomic force microscope. A549 cells were treated with or without 100 nm ND particles (100 μg/mL for 4 h) and simultaneously observed by Bio-AFM. The deflection and high-measured images of Bio-AFM showed the contour of the membrane surrounding of an ND-untreated A549 cell (Fig. 1, upper pictures). The macropinocytosis mediated by filopodia from cell-surface ruffling and extension that formed in the ND-treated cell (Fig. 1, lower picture, the arrows). ND particles (Fig. 1, the stars) were contacted with filopodia to help ND's uptake into cell. To further investigate the endocytosis of ND particles, transmission electron microscope (TEM) was used to examine the location of ND particles inside cell. As shown from the TEM images, ND particles can be found in the surrounding cell membrane or ingested into cell (Fig. 2A, dark black spots). A filopodium of cell membrane extension (Fig. 2B, the arrow) and membrane ruffling and invagination were formed for ND's uptake (Fig. 2B, the stars). An endocytic ND vesicle was formed inside of cell (Fig. 2C, the arrow). These ND's particles are located in cytoplasm but not nucleus. ND particles were accumulated to develop a single ND's cluster, which contained several ND particles (Fig. 2D). In addition to macropinocytosis, we examined clathrin-dependent endocytosis pathway for ND's entrance. As illustrated in Fig. 3A, the red color (Cy3) indicated the location of clathrin proteins, and the nuclei were stained with Hoechst 33258 that presented with blue color. The right picture of Fig. 3A indicated ND particles under phase contrast microscope observation. The magnified picture showed clathrin vesicles or cages that were formed in the ND-treated A549 cells (Fig. 3B, the arrows).

3.2. ND particles do not alter the cell growth ability and cell cycle progression

A549 and 3T3-L1 cells were treated with 100 nm ND particles (100 μg/mL for 48 h) and then re-cultured for 10 days. The total

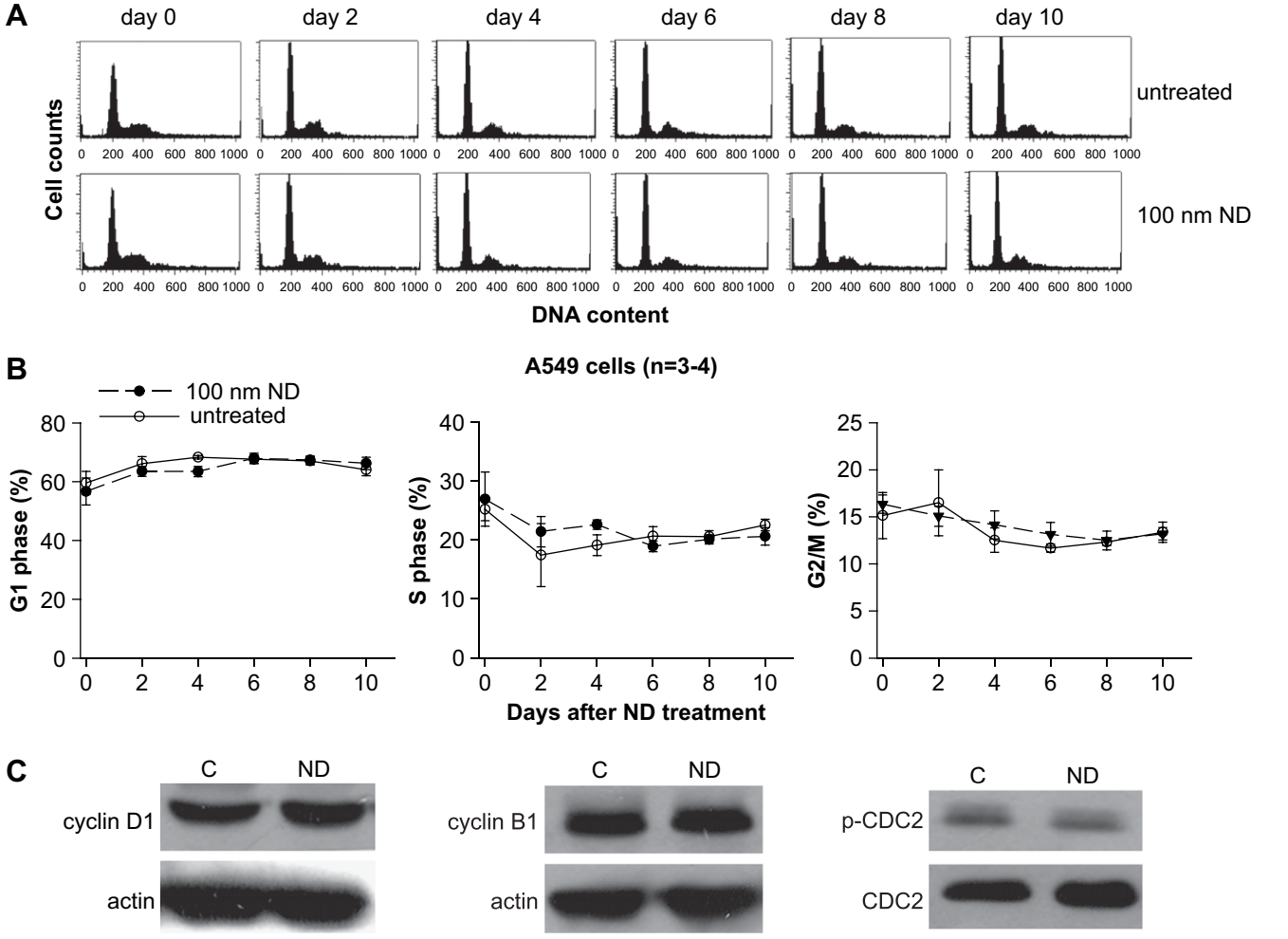

Fig. 5. The long-term effect of ND particles on cell cycle progression. (A) A549 cells were treated with or without 100 nm NDs (100 μg/mL for 48 h). After treatment, these cells were re-cultured in fresh medium and then were harvested by every 2 days until total 10 days. The cells were subjected to flow cytometer analysis. (B) The cell cycle phases including G1, S, and G2/M were quantified by a ModFit LT software of flow cytometer. Results were obtained from 3 to 4 separate experiments and the *bar* represents the mean ± S.E. (C) After treatment with or without ND particles (100 μg/mL for 48 h) in A549 cells, total protein extracts were prepared for Western blot analysis using specific cyclin D1, cyclin B1, phospho-CDC2 (threonine-161), CDC2, and actin antibodies. Western blot data were shown from one of three separate experiments with similar findings.

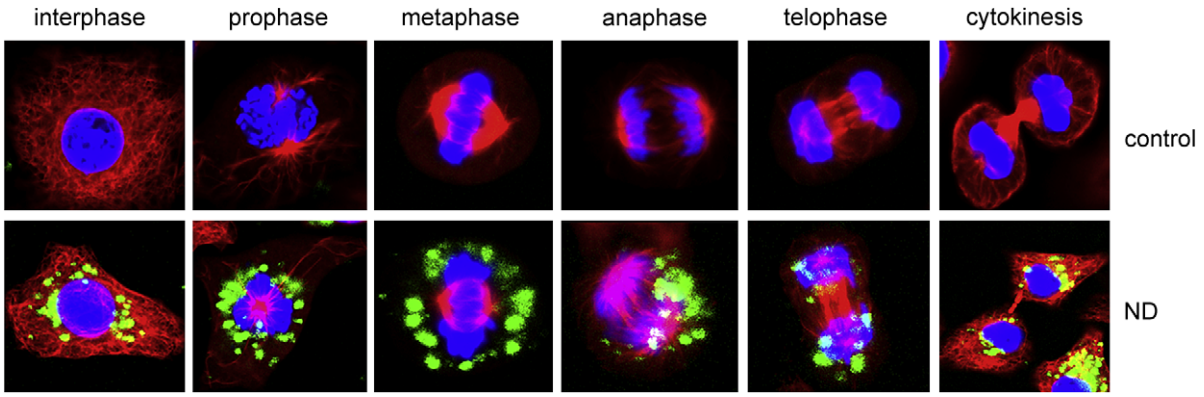

Fig. 6. The detection and distribution of ND particles in mitosis. A549 cells were incubated with or without 100 μg/mL ND particles for 48 h, and then replaced fresh medium for re-cultured 24 h. At the end of incubation, the cells were subjected to nuclear and microtubule staining, and observed by laser scanning confocal microscope. The microtubule was stained with anti-β-tubulin Cy3 that presented with red color. The nuclei were stained with Hoechst 33258 that presented with blue color. The green fluorescence from ND's particles was excited with wavelength 488 nm and the emission was collected in the range of 510–530 nm. ND particles were located in interphase and mitotic phases (prophase, metaphase, and telophase). During cytokinesis, these ND's particles were separated into two daughter cells.

cell number and cell cycle progression were analyzed by every 2 days up to total 10 days. It is found that ND particles did not alter the cell growth ability in both A549 (Fig. 4A) and 3T3-L1 (Fig. 4B) cells after long-term culture for 10 days. Subsequently, the effects of ND particles on cell cycle progression were analyzed by a flow cytometer. ND particles did not alter the cell cycle progression in A549 cells after long-term cell culture (Fig. 5A). The percentages of cell cycle phases (G1, S, and G2/M) were quantified by ModFit LT software of flow cytometer. The percentages in each phase were not altered by exposure to ND particles (no significant differences, $p > 0.05$) (Fig. 5B). The cell cycle-regulated proteins were examined by Western blot analysis using specific antibodies

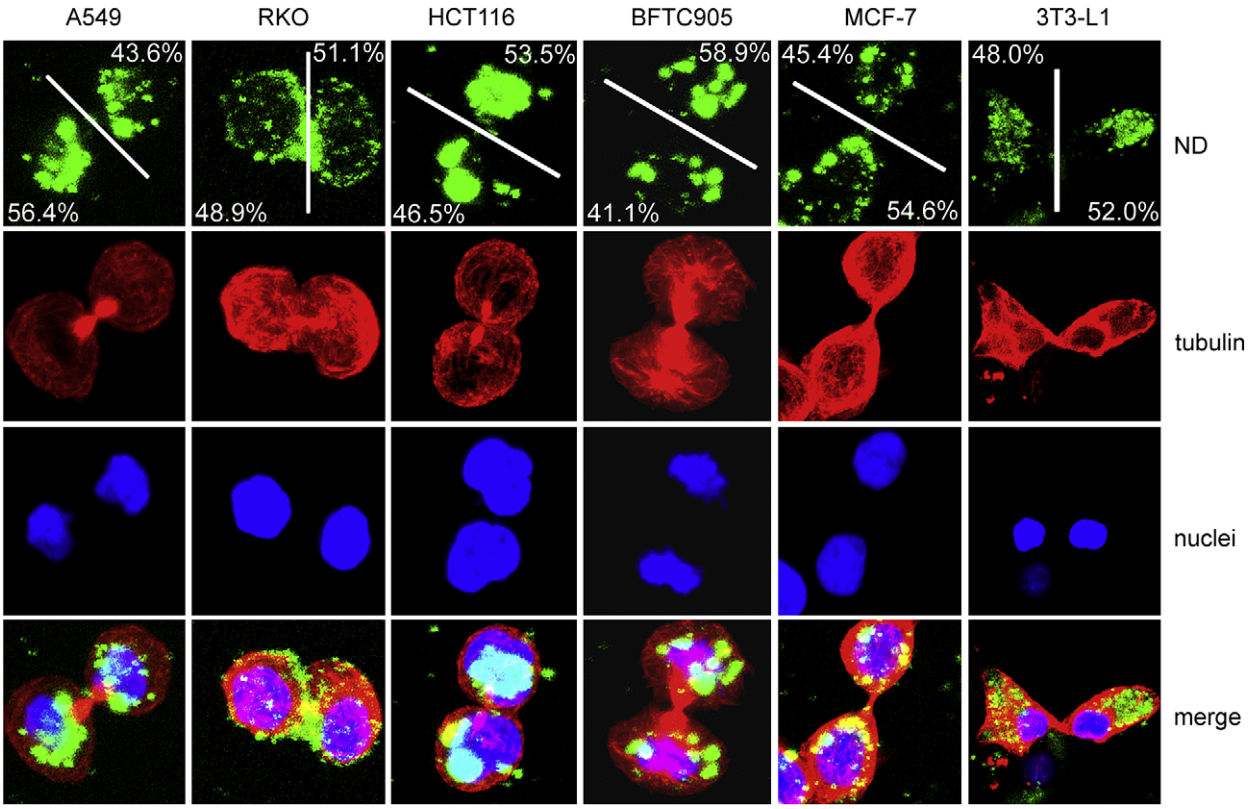

Fig. 7. The separation of ND particles in variety of cell lines during cytokinesis. (A) A549 cells were incubated with or without 100 μg/mL ND particles for 48 h, and then replaced fresh medium for re-cultured 24 h. At the end of incubation, the cells were subjected to nuclear and microtubule staining, and observed by laser scanning confocal microscope. The microtubule was stained with anti-β-tubulin Cy3 that presented with red color. The nuclei were stained with Hoechst 33258 that presented with blue color. The green fluorescence from ND's particles was excited with wavelength 488 nm and the emission was collected in the range of 510–530 nm. ND particles were located in interphase and mitotic phases (prophase, metaphase, and telophase). During cytokinesis, these ND's particles were separated into two daughter cells. (B) A variety of cancer cell lines including human lung (A549), colorectal (RKO and HCT116), bladder (BFTC905), breast (MCF-7) cancer cell lines, and mouse 3T3-L fibroblast were incubated with 100 nm ND particles (100 μg/mL for 48 h), and then replaced fresh medium for re-cultured 24 h. After incubation, the cells were subjected to nuclear and microtubule staining. The ratios of the green fluorescence intensities of ND's particles in separating daughter cells were quantified in each cell line.

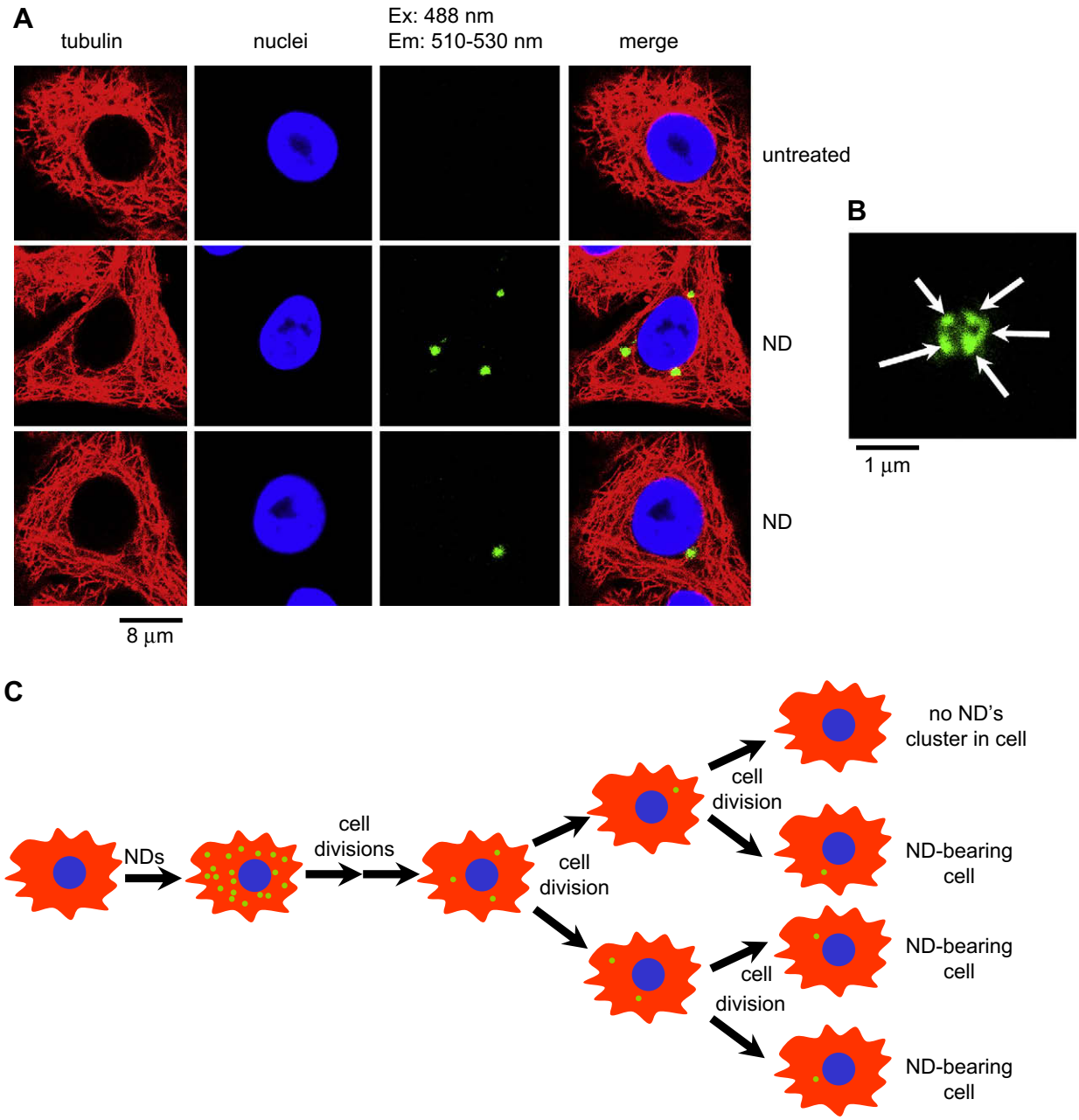

Fig. 8. Single ND's clusters located in cytoplasm after cell sub-cultured for several generations. (A) After treatment with or without 100 nm ND particles (100 μg/mL for 48 h), A549 cells were re-cultured in fresh medium for long-term examination until 10 days. At the end of incubation, the cells were subjected to nuclear and microtubule staining, and observed by laser scanning confocal microscope. The red fluorescence intensity exhibited by microtubule proteins of cytoskeleton, and the blue color indicated nuclei by staining with Hoechst 33258. One and three single ND's clusters (green color) were clearly presented in cells after cultured 10 days. These ND's clusters were located in the cytoplasm. (B) The amplified picture from (A) showed that a single ND's cluster contained 5 ND's particles (the arrows). (C) The model of a single ND's cluster carry in cell after sub-cultured for several cell generations.

cyclin D1, cyclin B1, phospho-CDC2 (threonine-161), CDC2, and actin. Actin protein is an internal control. Comparing with untreated samples, ND particles did not significantly alter the protein levels of cyclin D1, cyclin B1, phospho-CDC2 (threonine-161), and CDC2 (Fig. 5C).

3.3. Location and distribution of ND particles in cell division

To investigate the location and distribution of ND particles in cell division, the ND-treated cells were subjected to nuclear and microtubule staining, and observed by laser scanning confocal microscope. ND particles display natural green fluorescence upon laser excitation that can be detected by scanning confocal microscope (Fig. 6). Mitosis is sequencing order as spindle formation (red color) at prophase and metaphase, chromosome segregation (blue color) at anaphase, and separating two daughter cells at telophase and cytokinesis (Fig. 6). Interestingly, endocytic ND particles presented in all cell cycle phases, including interphase and mitotic phases (prophase, metaphase, and telophase) but did not disturb spindle formation and chromosome segregation (Fig. 6, lower panel). During cytokinesis, ND's particles were separated into two daughter cells (Fig. 6, lower panel). Moreover, ND's particles spread

in cytoplasm but not located in nucleus (interphase) or chromosomes (mitotic phases).

3.4. Separation of ND particles during cytokinesis in varying cancer cell lines and embryonic fibroblast

Varying cell types have been examined for illustrating universal of ND's uptake and their effects on cell division. Human cancer cell lines including human lung (A549), colorectal (RKO and HCT116), bladder (BFTC905), breast (MCF-7), and a mouse 3T3-L1 embryonic fibroblast were treated with ND particles (100 μg/mL for 48 h), and then replaced fresh medium for re-cultured 24 h. ND's particles were taken into all cell types (Fig. 7). Moreover, we have quantified the fluorescence intensities of ND particles in each cell line. The ratios of ND's particles were separated by 56.4%:43.6% (A549), 48.9%:51.1% (RKO), 46.5%:53.5% (HCT116), 41.1%:58.9% (BFTC905), 45.4%:54.6% (MCF-7) and 48.0%:52.0% (3T3-L1) in two daughter cells during cytokinesis (Fig. 7). Approximately, ND particles were separated equally into two daughter cells during cell division. One or three single ND's clusters (green color) were clearly presented in cells after sub-cultured for 10 days via several cell generations (Fig. 8A). The magnified picture showed a single ND's cluster, which contained ~5 ND particles (Fig. 8B, the arrows). We suggest a model that endocytic ND's clusters will be separated by cell division (Fig. 8C). Finally, the cell retained a single ND's cluster in cytoplasm after several cell generations.

3.5. Tracking of ND particles in 3T3-L1 adipogenic differentiation

To study the location and distribution of ND particles in cell differentiation, the adipogenic differentiation of mouse 3T3-L1 fibroblast was used in this study. Endocytic ND particles were retained inside of 3T3-L1 cells after cultured for 10 days (Fig. 9A, green color). Several single ND's clusters were formed in 3T3-L1 cells (Fig. 9B). Similar to A549 cells, these ND's clusters were located in cytoplasm but not nuclei in 3T3-L1 cells. The enlarged picture shows a single ND's cluster, which contained ~6 ND's particles (Fig. 9C, the arrows). Moreover, ND particles did not alter the level of cell cycle phases in 3T3-L1 cells (Fig. 9D). For adipogenic differentiation, the cells were incubated until confluent and then re-cultured in the differentiated DMEM medium, which contained differentiated promoting drugs including isobutyl-1-methylxanthine, dexamethasone, insulin, indomethacin, and roseglitazone. Adipogenic differentiation was assessed by the cellular accumulation of neutral lipid vacuoles by staining with oil-red O. 3T3-L1 cells were not differentiated when cultured in the drug-free DMEM medium (Fig. 10A and Fig. 10B). However, ND will be accumulated in 3T3-L1 cells by treatment with 100 nm ND particles (100 μg/mL for 48 h) (Fig. 10B, brown color). Neutral lipid vacuoles (red color) were highly presented in the differentiated adipocytes when cells incubated with differentiated DMEM medium. ND particles did not disturb the adipogenic differentiation of 3T3-L1 cells (Fig. 10D). The gene expressions (mRNA levels) of regulated adipogenic differentiation were analyzed by reverse transcription-polymerase chain

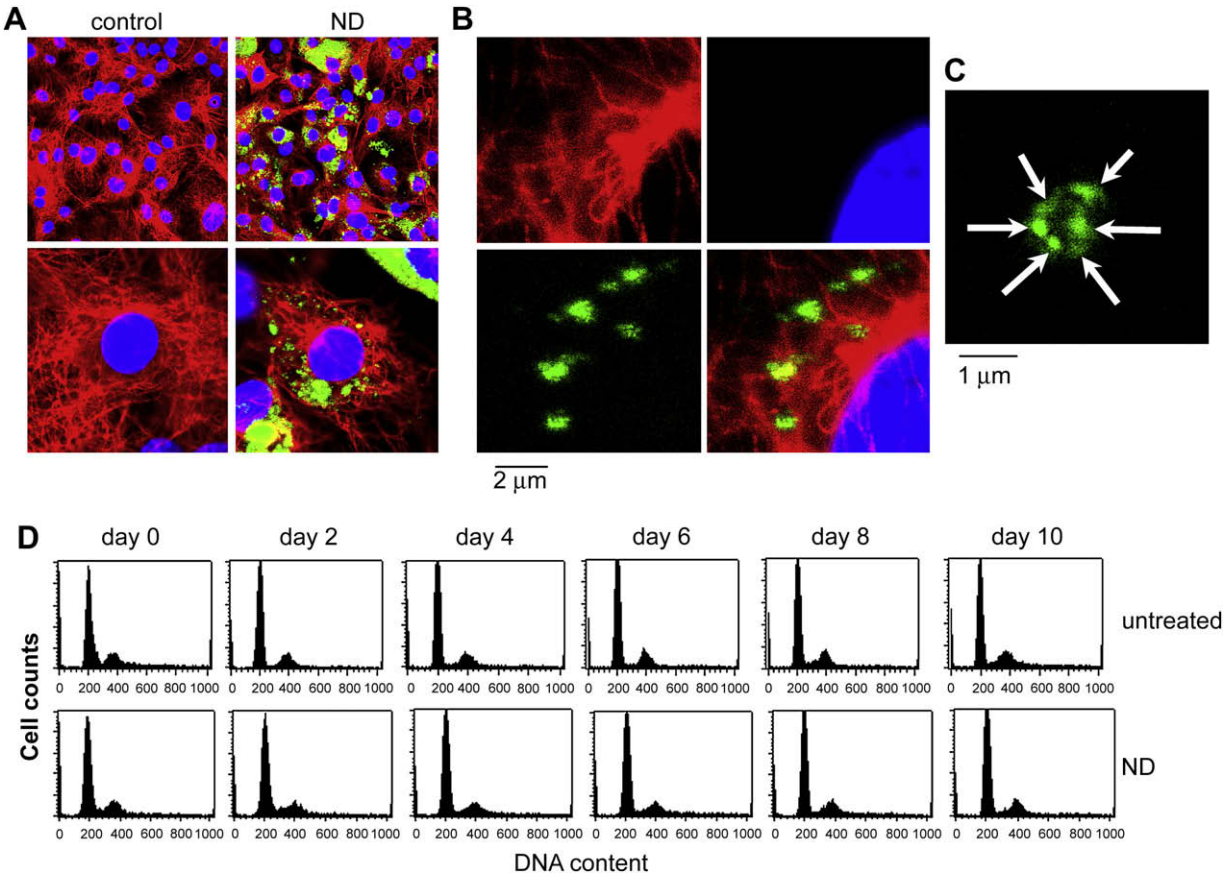

Fig. 9. The nanoparticle distribution and the effect on cell cycle progression following exposure to ND particles in 3T3-L1 cells. (A) After treatment with or without 100 nm ND particles (100 μg/mL for 48 h) in 3T3-L1, the cells were re-cultured in fresh medium for 10 days. The red fluorescence intensity exhibited by microtubule proteins of cytoskeleton, and the blue color indicated nuclei by staining with Hoechst 33258. The green fluorescence indicated the ND's particles. ND's particles were retained inside of cells after cultured 10 days. (B) Several single ND's clusters were formed and located in cytoplasm but not nucleus. (C) The amplified picture of a single ND's cluster from (B) showed that contained 6 ND's particles. (D) After treatment with or without 100 nm ND particles (100 μg/mL for 48 h), these cells were re-cultured in fresh medium, and analyzed by flow cytometry for cell cycle progression by every 2 days until 10 days.

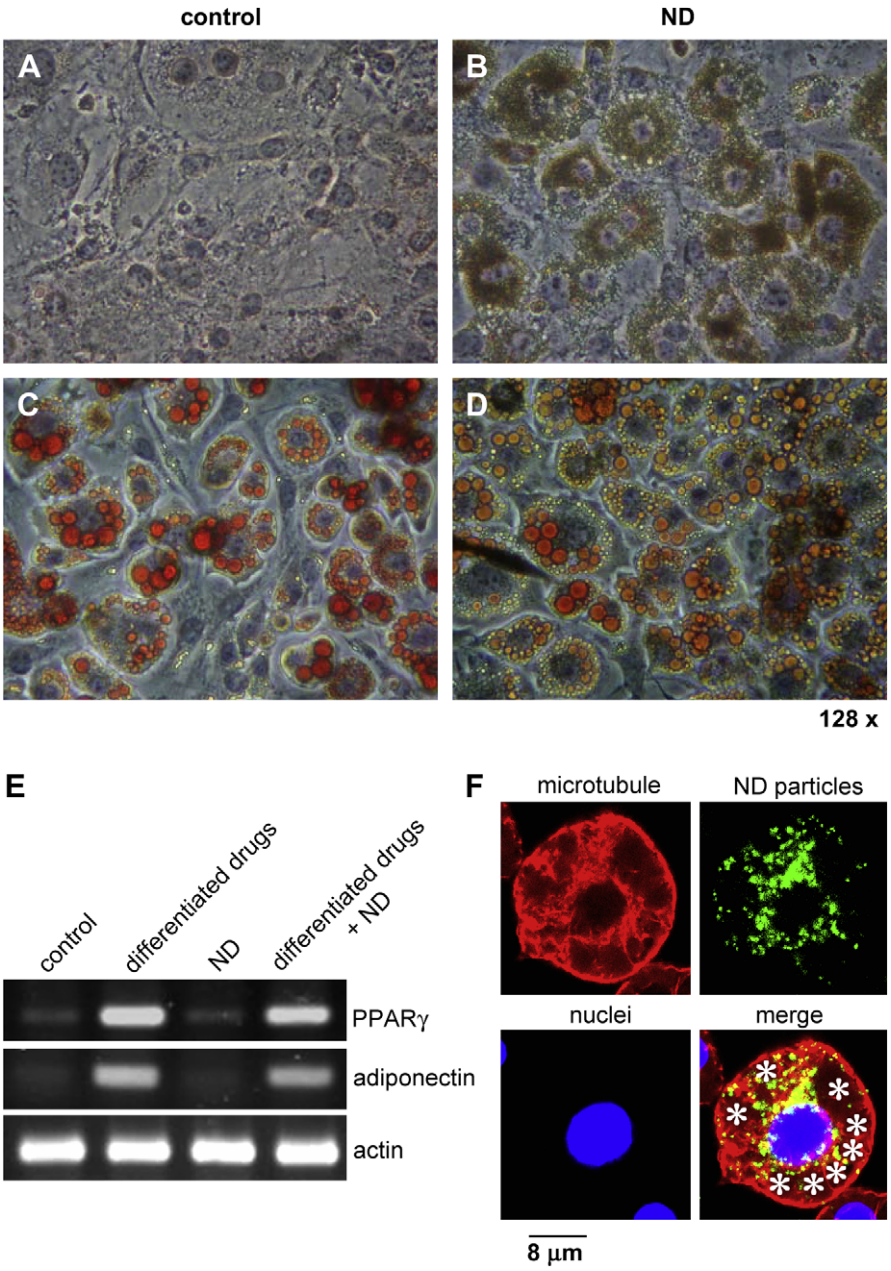

Fig. 10. The effect and distribution of ND particles in 3T3-L1 adipogenic differentiation. (A) and (B), 3T3-L1 cells were plated at a density of 1×10^6 cells per 100-mm Petri dish in DMEM medium. (C) and (D), 3T3-L1 cells were incubated until confluent and then re-cultured in differentiated DMEM medium, which supplemented differentiated drugs. 3T3-L1 fibroblasts were treated with (C) or without (D) 100 nm ND particles (100 μg/mL for 48 h) in the differentiated DMEM medium, and then the cells were re-cultured in fresh medium for 10 days. At the end of incubation, the cells were fixed and stained with oil-red O. Adipogenic differentiation was assessed by the cellular accumulation of neutral lipid vacuoles that observed under a phase contrast microscope. (E) 3T3-L1 fibroblasts were treated with or without 100 nm ND particles (100 μg/mL for 48 h) in control medium or the differentiated DMEM medium. Total cellular RNA was purified for reverse transcription-polymerase chain reaction (RT-PCR) analysis. The RT-PCR amplified gene products of PPARγ, adiponectin, and actin were 204, 243 and 544 bps, respectively. Actin is an internal control gene. (F) The lipid vacuoles were presented in a differentiated fat cell (the stars). The red fluorescence intensity exhibited by microtubule proteins of cytoskeleton. The blue color indicated nuclear staining by Hoechst 33258. The green fluorescence from the ND particles was excited with wavelength 488 nm and the emission was collected in the range of 510–530 nm.

reaction (RT-PCR). The RT-PCR amplification products of PPARγ, adiponectin, and actin were 204, 243 and 544 bps, respectively (Fig. 10E). Actin gene is a common internal control expressed in undifferentiated and differentiated cells. The mRNA levels of PPARγ and adiponectin were markedly increased when 3T3-L1 cells incubated with the differentiated medium (Fig. 10E). However, treatment with ND particles did not alter the mRNA levels of PPARγ and adiponectin in the adipogenic differentiation of mouse 3T3-L1 fibroblast (Fig. 10E). The ND particles were retained inside of a differentiated adipocyte after long-term cell culture for 10 days (Fig. 10F, green color). ND particles existed in cytoplasm but not in vacuoles (the stars) or nucleus (blue color) in differentiated fat cell (Fig. 10F).

4. Discussion

Development of a non-toxic and biocompatible nanomaterial has been highly desirable for biomedical applications. In this study, we provide that endocytic ND particles are non-cytotoxic in cell division and differentiation, which can be utilized for the

tracking of cancer and stem cells. It has been shown that ND particles do not induce cytotoxicity in lung [18], neuronal [19], renal [20,21], and cervical cells [22]; however, the short-term examinations (1–3 days) of ND particles were examined in these studies. We have further provided the 100 nm ND particles do not alter the cell growth ability and cell cycle progression for long-term observation (10 days). Accordingly, we suggest that ND is a promising non-cytotoxic carbon nanoparticle for biological applications.

The cell cycle progression mediated by appropriate activation of the cyclin-dependent protein kinases (CDKs) and cyclins for cell division and growth. CDK1 (CDC2) interacts with cyclin B1 that has been shown to play a critical role in the mitotic progression [23]. We found that 100 nm ND particles did not alter the cell cycle-regulated protein levels of cyclin D1, cyclin B1, phospho-CDC2 (threonine-161), and CDC2. Moreover, ND particles did not alter the total cell number and the percentage of cell cycle phases in both A549 and 3T3-L1 cells after long-term culture. The growth rate is relative quicker in A549 cells than 3T3-L1 cells (Fig. 4). It is possible that A549 is a lung cancer cell line, which displays highly proliferating in cell growth. 3T3-L1 is a normal fibroblast displayed slow growth rate in such condition. In addition, we also found that 5 nm ND particles did not alter the cell cycle progression in A549 cells (data not shown). The effect of ND particles on the adipogenic differentiation of mouse 3T3-L1 fibroblast was examined in this study. Cell differentiation is the specific process from progenitor or stem cells becoming another typing cell after stimulating with differentiated factors and genes [24,25]. Peroxisome proliferator-activated receptor gamma (PPARγ) is a lipid-activated transcription factor that promotes the adipogenesis of fibroblasts [25]. Adiponectin is a marker of differentiated adipocyte. ND's particles were retained inside of 3T3-L1 cells after cultured for 10 days. However, ND particles did not alter the mRNA levels of PPARγ and adiponectin in the adipogenic differentiation of mouse 3T3-L1 fibroblast. Thus, our results provide that these ND-bearing cells do not lose the cellular physiological functions on cell division and differentiation.

Subsequently, 100 nm ND particles can be taken into cells by macropinocytosis and clathrin-mediated endocytosis. The endocytic vesicles are generated differ in size and structure depending on different endocytosis pathways. We found the ND endocytic vesicle sizes that ranged from 0.2 μm to 1.0 μm. It has been proposed that the vesicle size is $<$1.0 μm (50–1000 nm) by macropinocytosis [13]. Moreover, the macropinocytosis mediated by filopodia from cell-surface ruffling and extension for ND's uptake into cells. In addition to macropinocytosis, we also found that clathrin-dependent endocytosis pathway mediated for ND's entrance. Clathrin is a three-legged structure, called a triskelion [15]. The clathrin-cage ($\sim$120 nm in diameter) assembly is required for clathrin-dependent endocytosis [13]. Accordingly, we suggest that 100 nm-sized ND particles can be taken into cell by both macropinocytosis and clathrin-dependent endocytosis. Previously, 5 nm ND particles were relative higher uptake ability than 100 nm ND particles [18]. We cannot exclude the caveolae-dependent uptake (vesicle size $\sim$60 nm) [16,17] and clathrin-/caveolae-independent endocytosis (vesicle size $\sim$90 nm) [13] that mediate ND's uptake by smaller size ($<$100 nm) ND particles. Therefore, the different size and modification of ND particles for entering cells need further investigation.

It is interested that endocytic ND's clusters can be formed in cytoplasm, which are not degradable and persistently existed inside cell without inducing cellular damages. Previously, we have shown that ND particles display natural green fluorescence upon laser excitation [18]. The location and distribution of ND particles in cell division and differentiation can be chased by laser scanning confocal microscope. Endocytic ND particles presented in mitosis but did not disturb spindle formation and chromosome segregation. Moreover, ND particles were separated into two daughter cells during cytokinesis. ND particles spread in cytoplasm but not located in nucleus or chromosomes. The findings indicate that ND particles do not induce the damages of chromosomes and microtubules. Finally, the cell retained a single ND's cluster, which contained 5–6 ND's particles in cytoplasm after sub-cultured for several cell divisions. Macropinosomes or endosomes will be formed by different endocytotic pathways, and further mature into and/or fuse with lysosomes for degradation of endocytic cargos [26,27]. Recently, Faklaris et al. have reported that ND particles are not trapped in endosomes [28]. Thus, we suggest that ND's clusters are not degradable and carry inside of cell. The ND-labeling cells can be developed the tracking for cancer or stem cells *in vitro* and *in vivo*.

5. Conclusions

ND particles can be taken into cell by both macropinocytosis and clathrin-mediated endocytosis. More importantly, endocytic ND particles do not disturb the cellular functions on cell division and differentiation. ND is a non-cytotoxic nanomaterial for the labeling and tracking of cancer and stem cells. Furthermore, the uptake ability of ND particles will provide the delivery of drugs, proteins, and nucleic acids for diagnostic and therapeutic applications.

Acknowledgements

This work was supported by grants from the National Science Council, Taiwan (NSC 96-2311-B-320-006-MY3, NSC 96-2113-M-259-001, NSC 97-2120-M-259-002) and partial financial support of National Chiao-Tung University. The authors wish to thank Tzu-Chi University (Hualien, Taiwan) for providing the use of TEM and Bio-AFM. In addition, we thank Professors C. C. Chang and K. C. Hwang for kindly providing discussions.

Appendix

Figures with essential colour discrimination. Figures 1, 3, and 6–10 in this article may be difficult to interpret in black and white. The full colour image can be found in the on-line version, at doi:10.1016/j.biomaterials.2009.04.056.

References

[1] Akerman ME, Chan WC, Laakkonen P, Bhatia SN, Ruoslahti E. Nanocrystal targeting in vivo. Proc Natl Acad Sci U S A 2002;99(20):12617–21.
[2] Dahan M, Levi S, Luccardini C, Rostaing P, Riveau B, Triller A. Diffusion dynamics of glycine receptors revealed by single-quantum dot tracking. Science 2003;302(5644):442–5.
[3] Michalet X, Pinaud FF, Bentolila LA, Tsay JM, Doose S, Li JJ, et al. Quantum dots for live cells, in vivo imaging, and diagnostics. Science 2005;307(5709):538–44.
[4] Farokhzad OC, Cheng J, Teply BA, Sherifi I, Jon S, Kantoff PW, et al. Targeted nanoparticle-aptamer bioconjugates for cancer chemotherapy in vivo. Proc Natl Acad Sci U S A 2006;103(16):6315–20.
[5] Chao JI, Perevedentseva E, Chung PH, Liu KK, Cheng CY, Chang CC, et al. Nanometer-sized diamond particle as a probe for biolabeling. Biophys J 2007;93(6):2199–208.
[6] Chang YR, Lee HY, Chen K, Chang CC, Tsai DS, Fu CC, et al. Mass production and dynamic imaging of fluorescent nanodiamonds. Nat Nanotechnol 2008;3(5):284–8.
[7] Balasubramanian G, Chan IY, Kolesov R, Al-Hmoud M, Tisler J, Shin C, et al. Nanoscale imaging magnetometry with diamond spins under ambient conditions. Nature 2008;455(7213):648–51.
[8] Neumann P, Mizuochi N, Rempp F, Hemmer P, Watanabe H, Yamasaki S, et al. Multipartite entanglement among single spins in diamond. Science 2008;320(5881):1326–9.

[9] Yang W, Auciello O, Butler JE, Cai W, Carlisle JA, Gerbi JE, et al. DNA-modified nanocrystalline diamond thin-films as stable, biologically active substrates. Nat Mater 2002;1(4):253–7.
[10] Cheng CY, Perevedentseva E, Tu JS, Chung PH, Chenga CL, Liu KK, et al. Direct and *in vitro* observation of growth hormone receptor molecules in A549 human lung epithelial cells by nanodiamond labeling. Appl Phy Lett 2007;90:163903.
[11] Liu KK, Chen MF, Chen PY, Lee TJF, Cheng CL, Chang CC, et al. Alpha-bungarotoxin binding to target cell in a developing visual system by carboxylated nanodiamond. Nanotechnology 2008;19:205102.
[12] Chithrani BD, Ghazani AA, Chan WC. Determining the size and shape dependence of gold nanoparticle uptake into mammalian cells. Nano Lett 2006;6(4):662–8.
[13] Conner SD, Schmid SL. Regulated portals of entry into the cell. Nature 2003;422(6927):37–44.
[14] Ridley AJ. Rho proteins: linking signaling with membrane trafficking. Traffic 2001;2(5):303–10.
[15] Schmid SL. Clathrin-coated vesicle formation and protein sorting: an integrated process. Annu Rev Biochem 1997;66:511–48.
[16] Pelkmans L, Helenius A. Endocytosis via caveolae. Traffic 2002;3(5):311–20.
[17] Drab M, Verkade P, Elger M, Kasper M, Lohn M, Lauterbach B, et al. Loss of caveolae, vascular dysfunction, and pulmonary defects in caveolin-1 gene-disrupted mice. Science 2001;293(5539):2449–52.
[18] Liu KK, Cheng CL, Chang CC, Chao JI. Biocompatible and detectable carboxylated nanodiamond on human cell. Nanotechnology 2007;18:325102.
[19] Schrand AM, Huang H, Carlson C, Schlager JJ, Omacr Sawa E, Hussain SM, et al. Are diamond nanoparticles cytotoxic? J Phys Chem B Condens Matter Mater Surf Interfaces Biophys 2007;111(1):2–7.
[20] Yu SJ, Kang MW, Chang HC, Chen KM, Yu YC. Bright fluorescent nanodiamonds: no photobleaching and low cytotoxicity. J Am Chem Soc 2005;127(50):17604–5.
[21] Lechleitner T, Klauser F, Seppi T, Lechner J, Jennings P, Perco P, et al. The surface properties of nanocrystalline diamond and nanoparticulate diamond powder and their suitability as cell growth support surfaces. Biomaterials 2008;29(32):4275–84.
[22] Chang IP, Hwang KC, Chiang CS. Preparation of fluorescent magnetic nanodiamonds and cellular imaging. J Am Chem Soc 2008;130(46):15476–81.
[23] Fang F, Newport JW. Evidence that the G1-S and G2-M transitions are controlled by different cdc2 proteins in higher eukaryotes. Cell 1991;66(4):731–42.
[24] Freytag SO, Geddes TJ. Reciprocal regulation of adipogenesis by Myc and C/EBP alpha. Science 1992;256(5055):379–82.
[25] Tontonoz P, Hu E, Spiegelman BM. Stimulation of adipogenesis in fibroblasts by PPAR gamma 2, a lipid-activated transcription factor. Cell 1994;79(7):1147–56.
[26] Berthiaume EP, Medina C, Swanson JA. Molecular size-fractionation during endocytosis in macrophages. J Cell Biol 1995;129(4):989–98.
[27] Ciechanover A. Proteolysis: from the lysosome to ubiquitin and the proteasome. Nat Rev Mol Cell Biol 2005;6(1):79–87.
[28] Faklaris O, Garrot D, Joshi V, Druon F, Boudou JP, Sauvage T, et al. Detection of single photoluminescent diamond nanoparticles in cells and study of the internalization pathway. Small 2008;4(12):2236–9.